

## AIR ENTRAINMENT IN CHUTE AND TUNNEL SPILLWAYS

Hubert CHANSON

Department of Civil Engineering  
 University of Queensland  
 QLD 4072, AUSTRALIA

### ABSTRACT

In supercritical open channel flows air is entrained at the free surface. This process is called self-aeration. A method to estimate the flow properties is presented. New results on drag reduction in self-aerated flows are developed. It is shown that the mechanisms of drag reduction are associated with the presence of an air concentration boundary layer next to the spillway invert. An analogy with dilute polymer solutions and microbubble modified boundary layers suggests that the presence of air next to the bottom increases the effective viscosity of the mixture and the sublayer thickness. In a second part self-aerated flow characteristics are discussed in the particular case of tunnel spillways.

### INTRODUCTION

For a spillway flow the upstream flow region is smooth and glassy. Next to the invert turbulence is generated and the boundary layer grows until the outer edge of the boundary layer reaches the surface (fig. 1). From this location, called the point of inception, the turbulent velocity acting next to the free surface can initiate natural free surface aeration. This process is called self-aeration. It was studied initially because the entrained air increases the bulk of the flow (FALVEY 1980). Further the presence of air reduces the friction losses (WOOD 1983). Also the presence of air in high velocity flows may be prevent or reduce the cavitation erosion damage to spillway surfaces (FALVEY 1990).

In the paper the characteristics of self-aerated flows are summarized in the first part. New results on drag reduction are presented. Then the flow properties are discussed in the particular case of a tunnel spillway.

### SELF-AERATED FLOW CHARACTERISTICS

#### Air Concentration and Velocity Distribution

In self-aerated flows, velocity measurements obtained on a prototype spillway (CAIN 1978) and on a spillway model (CHANSON 1988) indicate that the velocity distribution of the air-water mixture is not affected by the presence of air bubbles. It may be estimated by a power law :

$$\frac{V}{V_{90}} = \left[ \frac{y}{Y_{90}} \right]^{1/6} \quad (1)$$

where  $y$  is measured perpendicular to the spillway surface,  $V$  the velocity,  $Y_{90}$  the depth where the air concentration is 90% and  $V_{90}$  the velocity at  $Y_{90}$ . The air concentration

distribution can be represented by a diffusion model of the air bubbles within the air-water mixture (WOOD 1984) as :

$$C = \frac{B'}{B' + e^{-(G' \cos \alpha * y'^2)}} \quad (2)$$

where  $C$  is the air concentration defined as the volume of air per unit volume,  $B'$  and  $G'$  are functions of the mean air concentration only,  $\alpha$  is the slope and  $y' = y/Y_{90}$ . Values of  $B'$  and  $G'$  are deduced from table I, columns 2 and 3, as a function of the mean air concentration  $C_{mean}$ .

Next to the spillway bottom, the data of CAIN (1978) and CHANSON (1988) depart from equation (2) and indicate that the air concentration tends to zero at the bottom. This result is consistent with the data of BOGDEVICH et al. (1977), MADAVAN et al. (1984) and MARIE et al. (1991) who studied the injection of micro-air-bubbles in turbulent boundary layer flows. Their measurements of air bubble concentration distributions showed also that the bubble concentration falls off to zero at the boundary. A re-analysis of CAIN's and CHANSON's data shows consistently the presence of an air concentration boundary layer, in which the air concentration distribution may be estimated as :

$$C = k * \sqrt[3]{\frac{y}{\delta_{ab}}} \quad (3)$$

where  $\delta_{ab}$  is the air concentration boundary layer thickness, and  $k$  a constant that satisfies the continuity between equations (2) and (3). For CAIN's and CHANSON's data, the air concentration boundary layer thickness was 10 to 15 mm (table II).

For a given mean air concentration, the velocity  $V_{90}$  is deduced from the continuity equation. Results are given in table I, column 5. A reasonable correlation is :

$$V_{90} = \frac{q_w}{Y_{90} * (0.857 - 0.862 * C_{mean}^{0.89})} \quad (4)$$

where  $q_w$  is the water discharge per unit width.

#### Drag Reduction in Self-Aerated Flows

The presence of air bubbles does not affect the velocity distribution but is expected to reduce the shear stress between the flow layers. WOOD (1983) and later CHANSON (1992) showed that self-aeration induces a drag reduction which increases with the mean air concentration. An estimate of the drag reduction is :

$$\frac{f_e}{f} = 0.5 * \left[ 1 + \tanh \left[ 0.70 * \frac{0.490 - C_{mean}}{C_{mean} * (1 - C_{mean})} \right] \right] \quad (5)$$

where  $f$  is the non-aerated flow friction factor and  $f_e$  the aerated friction factor (table I, column 6).

The author re-analysed prototype data obtained in Australia, Austria, Indonesia, USA, USSR and Yugoslavia (table III). The results are presented in figure 2 and compared with equation (5). Figure 2 shows that the aerated friction factor  $f_e$  departs from the non aerated value  $f$  for mean air concentrations larger than 20% : i.e. when the air concentration next to the chute invert  $C_b$  becomes larger than zero and air bubbles start interacting with the shear layers next to the invert.

**Discussion.** An aspect of the drag reduction in self-aerated flows is the interactions between the velocity profile and the air concentration distribution next to the chute invert. By analogy with dilute polymer solutions (VIRK 1975, LUMLEY 1977) and micro-bubble-modified boundary layers (MADAVAN et al. 1984-85, MARIE 1987, MARIE et al. 1991), the air concentration boundary layer might play a role similar to the elastic sub-layer and viscous sublayer in the drag reduction process.

The presence of air bubbles next to a solid boundary increases the effective dynamic viscosity, resulting in a thickening of the viscous sublayer (LUMLEY 1977, MARIE 1987). In the flow layers close to the boundary, the effective density and viscosity of the air-water mixture are :  $\rho = \rho_w * (1 - C_b)$  and  $\mu = \mu_w * (1 + 2.5 * C_b)$  where  $C_b$  is the air concentration at the edge of the air concentration boundary layer,  $\rho_w$  the water density and  $\mu_w$  the water viscosity. MARIE (1987) developed an analytical model to estimate the drag reduction due to the presence of air bubbles next to the wall :

$$\frac{f_e}{f} = \left[ 1 + \sqrt{\frac{f}{8}} * \left( 10.5 * \left[ \frac{1+2.5*C_b}{1-C_b} - 1 \right] - 2.44 * \ln \left[ \frac{1+2.5*C_b}{1-C_b} \right] \right) \right]^{-9/5} \quad (6)$$

Equation (6) is plotted on figure 3 as a function of  $C_{mean}$  using the air concentration at the outer edge of the air concentration boundary layer  $C_b$  (table I, column 4). In the air concentration boundary layer, experimental data (CAIN 1978, CHANSON 1988) and calculations (CHANSON 1992) indicate that, next to the spillway invert, the bubble diameters are small (i.e.  $d_b < 1$  mm). These values are of the same order of magnitude as the experiments of MADAVAN et al. (1984,1985) used to verify MARIE's (1987) model. Comparison between equations (5) and (6) is presented on figure 3. The agreement between these equations is good and confirms the analogy in the mechanisms of drag reduction.

In a more descriptive manner, the small air bubbles observed in the air concentration boundary layer act as rigid spheres and offer a large resistance to break up under the action of turbulent shear stress. Such rigid air bubbles behave as macro-molecules of polymer and block the turbulence bursting processes in the air concentration boundary layer as macro-molecules do in the viscous sub-layer (VIRK 1975). Dilute polymer solutions can exhibit macromolecular elongation characteristics that induces an increase of viscosity in the outer region of the sublayer called the elastic sublayer (VIRK 1975, TAM et al. 1992). In self-aerated flows the presence of air bubbles at the outer edge of the air concentration boundary layer is similar to the presence of

Table I - Air concentration and velocity distribution parameters in self-aerated flows

$C_{mean}$	$G'^*$ $\cos \alpha$	$B'$	$C_b$	$V_{90} * Y_{90}$ $q_w$	$f_e/f$ Eq. (5)
(1)	(2)	(3)	(4)	(5)	(6)
0.0	+infinite	0.0	0.00	1.167	1.0
0.161	7.999	0.00302	0.02	1.453	0.968
0.241	5.744	0.02880	0.04	1.641	0.870
0.310	4.834	0.07157	0.07	1.805	0.765
0.410	3.825	0.19635	0.17	2.141	0.613
0.569	2.675	0.62026	0.36	2.985	0.389
0.622	2.401	0.8157	0.46	3.319	0.313
0.680	1.8942	1.3539	0.55	4.151	0.228
0.721	1.5744	1.8641	0.64	4.859	0.167

Table II - Air concentration boundary layer characteristics

Reference	$\delta_{ab}$ mm	Bubble size $d_b$ mm	$C_b$	$V$ m/s	Comments
(1)	(2)	(3)	(4)	(5)	(6)
MADAVAN et al. (1984)		0.005		4 to 17	Microbubble-modified boundary layer
MADAVAN et al. (1985)		0.0005 to 0.1		4 to 17	Microbubble-modified boundary layer
MARIE et al. (1991)	2	4	0.02 to 0.07	0.5 to 1	Bubbly boundary layer on a flat plate.
CAIN (1978)	10 to 15	0.5 to 5	0 to 0.4	18 to 22	Prototype spillway.
CHANSON (1988)	10 to 15	0.3 to 4	0 to 0.2	9 to 17	Spillway model.

elongated macromolecules in the elastic sublayer. Air bubbles and elongated macromolecules increase the viscosity and "this increase in viscosity, in the turbulent part and not in the viscous sublayer, suppresses the eddies which carries the Reynolds stress in the buffer layer, resulting in a thickening of the sublayer, and a reduction in drag" (LUMLEY 1977).

## SELF-AERATED FLOW IN TUNNEL SPILLWAY

Above the air-water interface of self-aerated flows, an air boundary layer develops (JEVDJEVICH and LEVIN 1953). In tunnel spillways the interactions between the roof of the tunnel and the air boundary layer reduce the amount of air available and the air entrainment process. Further, if the air flow cross-sectional area is less than 5% of the total tunnel cross-section area, the free surface flow would disappear (CHEPAIKIN and DONCHENKO 1984).

A re-analysis of experimental measurements obtained by VOLKART (1982) in partially filled circular pipes and VOLKART and RUTSCHMANN (1984) in a rectangular tunnel spillway, shows that the ratio of entrainment velocity in tunnel spillway over entrainment velocity in chute spillway is in the range 0.4 to 0.6. In a tunnel spillway, the amount of air available above the free surface is limited. Further as the air flow is accelerated, the air pressure decreases along the spillway. The air entrainment process is expected to be reduced compared with a chute spillway flow situation.

### Air flow in tunnel spillway

The mass of air is 1000 times less than the mass of water and cannot substantially affect the velocity of the air-

Table III - Self-aerated flow measurements on prototype and model spillways

Spillway	$\alpha$ degrees	$q_w$ m <sup>2</sup> /s	Ref.	Comments
(1)	(2)	(3)	(4)	(5)
<b>Prototype spillways</b>				
Ak-Tepe, USSR	21.8	2.3 to 8.0	[A]	Rough concrete. W = 5 m. $k_s = 5$ mm.
Aviemore, NZ	45.0	2.23 & 3.16	[CA]	Concrete. $k_s = 1$ mm.
Bencok, Indonesia	31.05	2.9 to 6.0	[A,E,L]	W = 1 m. $k_s = 2$ mm.
Big Hill, Australia	4.2	0.74 to 0.82	[M]	Smooth concrete.
Dago, Indonesia	13.8	0.74 to 1.39	[A,E,L]	W = 1 m. $k_s = 1$ mm.
Erevan, USSR	21.8	0.38 to 1.55	[A]	Rough basalt. W=4 m. $k_s=10$ mm.
Gizel'don, USSR	28.1	0.49 to 1.28	[A]	Wooden flume. W = 6 m. $k_s = 0.3$ mm.
Hat Creek, USA	23.4 to 34.8	1.86 to 6.4	[H]	Rough concrete. W = 1.75 m. $k_s = 5$ mm.
Kittitas, USA	33.2	2.24 to 11.7	[H]	Eroded concrete. W = 2.44 m. $k_s = 10$ mm.
Mallnitz, Austria	22.2		[A,E,L]	Concrete. W = 2m.
Mostarsko Blato, Yugoslavia		0.71 to 3.44	[J]	Stone lining. W = 5.35 m. $k_s = 20$ mm.
Rapid Flume, USA	20.1	1.76	[H]	Wooden flume. W = 1.4 m. $k_s = 0.1$ mm.
Spring Gully, Australia	5.3		[M]	Smooth concrete. Semi circular (R=0.61 m).
Rutz, Austria	34	0.4 to 2	[I]	Concrete. Trapezoidal.
<b>Spillway models</b>				
Clyde model, NZ	52.3	0.21 to 0.48	[CH]	Perspex. D/S of aerator. W=0.25 m.
IWP, USSR	16.7 & 29.7	0.064 to 0.13	[A]	Planned board with painting. W=0.25 m.
Vienna Lab., Austria	8.7 to 31.2	0.04 to 0.18	[A,E,J,L]	Wooden flume. W=0.25 m.
St Anthony Falls, USA	7.5 to 75	0.14 to 0.93	[S]	Artificial roughness. W=0.46 m. $k_s=0.7$ mm.

Notes : [A] AIVAZYAN (1986); [CA] CAIN (1978); [CH] CHANSON (1988); [E] EHRENBERGER (1926); [H] HALL (1943); [I] INNEREBNER (1924); [J] JEVDJEVICH and LEVIN (1953) [L] LEVIN (1955); [M] MICHELS and LOVELY (1953); [S] STRAUB and ANDERSON (1958)

water flow. The air flow can be regarded as a Couette flow between a movable air-water boundary and a stationary solid boundary. In uniform flows and defining the air-water interface as  $y = Y_{90}$ , the mean air flow velocity equals approximately half of the interface velocity  $V_{90}$ . The total amount of air flowing in the tunnel spillway  $q_{air}^{total}$  equals the amount of air entrained by self-aeration plus the air flow above the free surface. For a rectangular tunnel it yields:

$$\frac{q_{air}^{total}}{q_w} = \frac{C_{mean}}{1 - C_{mean}} + \frac{\frac{1}{2} * \left( \frac{H}{Y_{90}} - 1 \right)}{0.857 - 0.862 * C_{mean}^{0.89}} \quad (7)$$

In steep tunnel spillways, the air-water flow is accelerated along the spillway and the velocity  $V_{90}$  increases as the flow depth decreases. If uniform flow conditions are reached, the total air discharge in the tunnel can be estimated from equation (7). When designing a tunnel spillway, the total air flow, taking into account self-aeration, must be less than the maximum flow rate at the intake of the tunnel. To a first approximation and neglecting the effects of compressibility, the maximum air flow rate at the start of a rectangular tunnel spillway equals :

$$q_{air}^{max} = \sqrt{\gamma * R * T * (H - d_0)} \quad (8)$$

where  $d_0$  is the initial flow depth, T the temperature,  $\gamma$  the specific heat ratio and R the gas constant. Neglecting the effects of compressibility, comparing equations (7) and (8) provides a simple method to estimate the need of additional air vents.

## CONCLUSION

The characteristics of self-aerated flows are developed for chute spillways. Although the velocity distribution is not affected by the presence of air bubbles, the shape of the air

concentration distribution shows the presence of an air concentration boundary layer that might play a major role in the drag reduction process. By analogy with dilute polymer solutions and microbubble modified boundary layers, it is suggested that the presence of air next to the invert increases the effective viscosity of the mixture and the sublayer thickness, and induces drag reduction as observed on prototype (fig. 2). In tunnel spillways, the interactions between the air boundary layer above the flow and the roof affect the air entrainment processes. At the present time, an insufficient number of data is available and additional work is required.

## REFERENCES

- AIVAZYAN, O.M. (1986). "Stabilized Aeration on Chutes." *Gidrotekhnicheskoe Stroitel'stvo*, No. 12, pp. 33-40.
- BOGDEVICH, V.G., EVSEEV, A.R., MLYUGA, A.G., and MIGIRENKO, G.S. (1977). "Gas-Saturation Effect on Near-Wall Turbulence Characteristics." *2nd Intl. Conf. on Drag Reduction*, BHRA Fluid Eng., Cambridge, UK, p. 25.
- CAIN, P. (1978). "Measurements within Self-Aerated Flow on a Large Spillway." Ph.D. Thesis, Uni. of Canterbury, New Zealand.
- CHANSON, H. (1988). "A Study of Air Entrainment and Aeration Devices on a Spillway Model." Research Rep. 88-8, Uni. of Canterbury, New Zealand.
- CHANSON, H. (1992). "Air Entrainment in Chutes and Spillways." Research Report No. CE 133, Dept. of Civil Eng., Univ. of Queensland, Australia.
- CHEPAIKIN, G.A., and DONCHENKO, E.G. (1986). "Certain Effects of Flow Aeration in Spillways." *Gidrotekhnicheskoe Stroitel'stvo*, No. 11, pp. 19-22.
- EHRENBERGER, R. (1926). "Wasserbewegung in steilen Rinnen (Susstennen) mit besonderer Berücksichtigung der Selbstbelüftung." *Zeitschrift des Österreichischer Ingenieur und Architektverein*, No. 15/16 and 17/18.

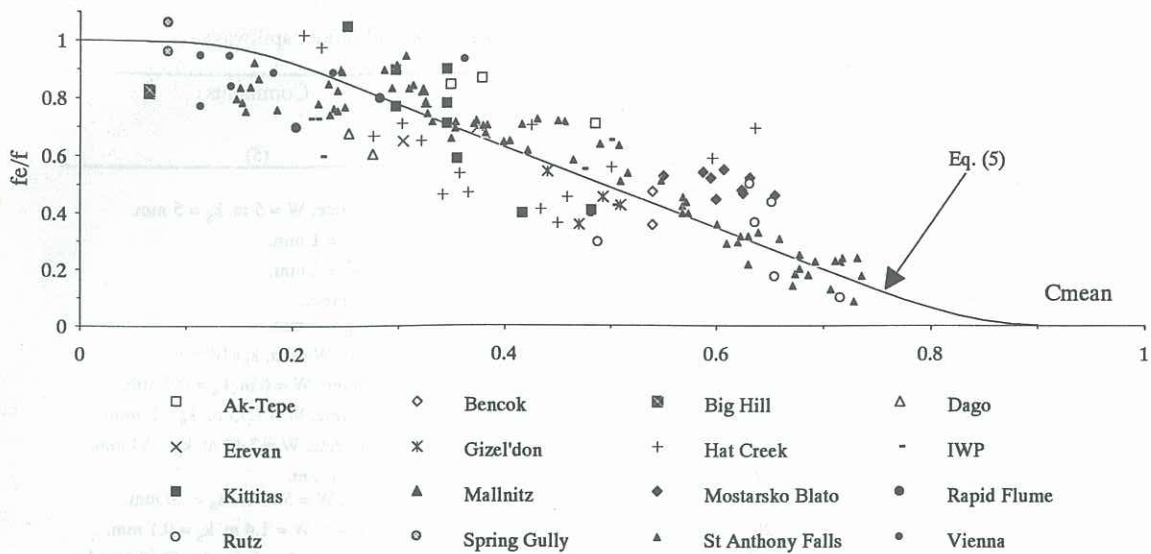


Fig. 2 - Drag reduction on prototype and model spillways

FALVEY, H.T. (1980). "Air-Water Flow in Hydraulic Structures." USBR Monograph, No. 41, Denver, USA.

FALVEY, H.T. (1990). "Cavitation in Chutes and Spillways." USBR Monograph, No. 42, Denver, USA.

INNEREBNER, K. (1924). "Overflow Channels from Surge Tanks." World Power Conference, 1st, Vol. 2, p. 481.

JEVDEJEVICH, V., and LEVIN, L. (1953). "Entrainment of Air in flowing Water and Technical Problems connected with it." 5th IAHR Congress, IAHR-ASCE, Minneapolis, USA, pp. 439-454.

LEVIN, L. (1955). "Quelques Réflexions sur la Mécanique de l'écoulement des Mélanges d'Eau et d'Air." La Houille Blanche, No. 4, pp. 55-557.

LUMLEY, J.L. (1977). "Drag Reduction in Two Phase and Polymer Flows." Physics Fluids, Vol. 20, No. 10, Pt II, pp. S64-S71.

MADAVAN, N.K., DEUTSCH, S., and MERKLE, C.L. (1984). "Reduction of Turbulent Skin Friction by Microbubbles." Physics Fluids, Vol. 27, No. 2, pp. 356-363.

MADAVAN, N.K., DEUTSCH, S., and MERKLE, C.L. (1985). "Measurements of Local Skin Friction in a Microbubble-Modified Turbulent Boundary Layer." Jl Fluid Mech., Vol. 156, pp. 237-256.

MARIE, J.L. (1987). "A Simple Analytical Formulation for Microbubble Drag Reduction." PCH, Vol. 8, No. 2, pp. 213-220.

MARIE, J.L., MOURSALI, E., and LANCE, M. (1991). "A First Investigation of a Bubbly Boundary Layer on a Flat Plate : Phase Distribution and Wall Shear Stress Measurements." 1st ASME-JSME Fluids Eng. Conf., ASME, Portland, USA, FED-Vol. 110, pp. 75-80.

MICHELS, V., and LOVELY, M. (1953). "Some Prototype Observations of Air Entrained Flow." 5th IAHR Congress, IAHR-ASCE, Minneapolis, USA, p. 403.

STRAUB, L.G., and ANDERSON, A.G. (1958). "Experiments on Self-Aerated Flow in Open Channels." Jl of Hyd. Div., Proc. ASCE, Vol. 84, No. HY7, paper 1890.

TAM, K.C., TIU, C., and KELLER, R.J. (1992). "A General Correlation for Turbulent Velocity Profiles of Dilute Polymer Solutions." Jl of Hyd. Res., Vol. 30, No. 1, p. 117.

VIRK, P.S. (1975). "Drag Reduction Fundamentals." AIChE Jl, Vol. 21, No. 4, pp. 625-656.

VOLKART, P. (1982). "Self-Aerated Flow in Steep,

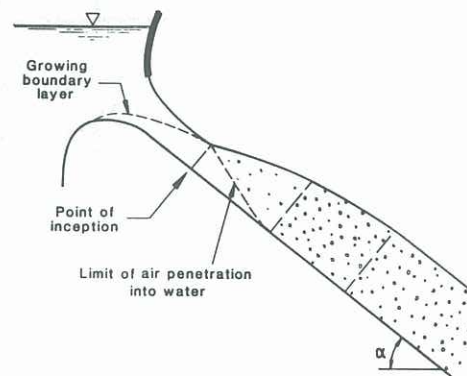


Fig. 1 - Air entrainment along a spillway

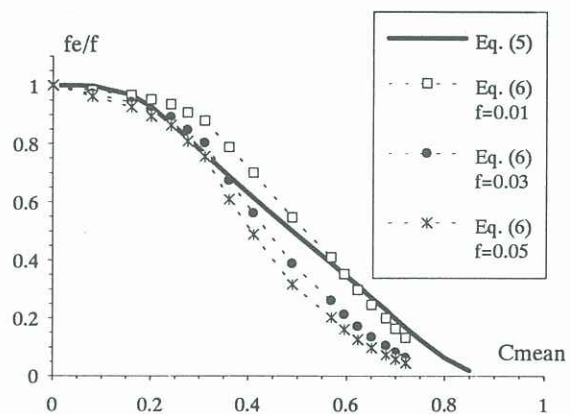


Fig. 3 - Comparison between equations (5) and (6)

Partially Filled Pipes." Jl of Hyd. Div., ASCE, Vol. 108, No. HY9, pp. 1029-1046.

VOLKART, P., and RUTSCHMANN, P. (1984). "Rapid Flow in Spillway Chutes with and without Deflectors - A Model-Prototype Comparison." Intl. Symp. on Scale Effects in Modelling Hydraulic Structures, IAHR, Esslingen, Germany, paper 4.5.

WOOD, I.R. (1983). "Uniform Region of Self-Aerated Flow." Jl Hyd. Eng., ASCE, Vol. 109, No. 3, pp. 447-461.

WOOD, I.R. (1984). "Air Entrainment in High Speed Flows." Intl. Symp. on Scale Effects in Modelling Hydraulic Structures, IAHR, Esslingen, Germany, paper 4.1.

Table III - Self-aerated flow measurements on prototype and model spillways

Spillway	$\alpha$ degrees	$q_w$ m <sup>2</sup> /s	Ref.	Comments
(1)	(2)	(3)	(4)	(5)
<b>Prototype spillways</b>				
Ak-Tepe, USSR	21.8	2.3 to 8.0	[A]	Rough concrete. W = 5 m. $k_s = 5$ mm.
Aviemore, NZ	45.0	2.23 & 3.16	[CA]	Concrete. $k_s = 1$ mm.
Bencok, Indonesia	31.05	2.9 to 6.0	[A,E,L]	W = 1 m. $k_s = 2$ mm.
Big Hill, Australia	4.2	0.74 to 0.82	[M]	Smooth concrete.
Dago, Indonesia	13.8	0.74 to 1.39	[A,E,L]	W = 1 m. $k_s = 1$ mm.
Erevan, USSR	21.8	0.38 to 1.55	[A]	Rough basalt. W=4 m. $k_s=10$ mm.
Gizel'don, USSR	28.1	0.49 to 1.28	[A]	Wooden flume. W = 6 m. $k_s = 0.3$ mm.
Hat Creek, USA	23.4 to 34.8	1.86 to 6.4	[H]	Rough concrete. W = 1.75 m. $k_s = 5$ mm.
Kittitas, USA	33.2	2.24 to 11.7	[H]	Eroded concrete. W = 2.44 m. $k_s = 10$ mm.
Mallnitz, Austria	22.2		[A,E,L]	Concrete. W = 2m.
Mostarsko Blato, Yugoslavia		0.71 to 3.44	[J]	Stone lining. W = 5.35 m. $k_s = 20$ mm.
Rapid Flume, USA	20.1	1.76	[H]	Wooden flume. W = 1.4 m. $k_s = 0.1$ mm.
Spring Gully, Australia	5.3		[M]	Smooth concrete. Semi circular (R=0.61 m).
Rutz, Austria	34	0.4 to 2	[I]	Concrete. Trapezoidal.
<b>Spillway models</b>				
Clyde model, NZ	52.3	0.21 to 0.48	[CH]	Perspex. D/S of aerator. W=0.25 m.
IWP, USSR	16.7 & 29.7	0.064 to 0.13	[A]	Planned board with painting. W=0.25 m.
Vienna Lab., Austria	8.7 to 31.2	0.04 to 0.18	[A,E,J,L]	Wooden flume. W=0.25 m.
St Anthony Falls, USA	7.5 to 75	0.14 to 0.93	[S]	Artificial roughness. W=0.46 m. $k_s=0.7$ mm.

Notes : [A] AIVAZYAN (1986); [CA] CAIN (1978); [CH] CHANSON (1988); [E] EHRENBERGER (1926); [H] HALL (1943); [I] INNEREBNER (1924); [J] JEVDJEVICH and LEVIN (1953) [L] LEVIN (1955); [M] MICHELS and LOVELY (1953); [S] STRAUB and ANDERSON (1958)

water flow. The air flow can be regarded as a Couette flow between a movable air-water boundary and a stationary solid boundary. In uniform flows and defining the air-water interface as  $y = Y_{90}$ , the mean air flow velocity equals approximately half of the interface velocity  $V_{90}$ . The total amount of air flowing in the tunnel spillway  $q_{air}^{total}$  equals the amount of air entrained by self-aeration plus the air flow above the free surface. For a rectangular tunnel it yields:

$$\frac{q_{air}^{total}}{q_w} = \frac{C_{mean}}{1 - C_{mean}} + \frac{\frac{1}{2} * \left( \frac{H}{Y_{90}} - 1 \right)}{0.857 - 0.862 * C_{mean}^{0.89}} \quad (7)$$

In steep tunnel spillways, the air-water flow is accelerated along the spillway and the velocity  $V_{90}$  increases as the flow depth decreases. If uniform flow conditions are reached, the total air discharge in the tunnel can be estimated from equation (7). When designing a tunnel spillway, the total air flow, taking into account self-aeration, must be less than the maximum flow rate at the intake of the tunnel. To a first approximation and neglecting the effects of compressibility, the maximum air flow rate at the start of a rectangular tunnel spillway equals :

$$q_{air}^{max} = \sqrt{\gamma * R * T * (H - d_0)} \quad (8)$$

where  $d_0$  is the initial flow depth, T the temperature,  $\gamma$  the specific heat ratio and R the gas constant. Neglecting the effects of compressibility, comparing equations (7) and (8) provides a simple method to estimate the need of additional air vents.

## CONCLUSION

The characteristics of self-aerated flows are developed for chute spillways. Although the velocity distribution is not affected by the presence of air bubbles, the shape of the air

concentration distribution shows the presence of an air concentration boundary layer that might play a major role in the drag reduction process. By analogy with dilute polymer solutions and microbubble modified boundary layers, it is suggested that the presence of air next to the invert increases the effective viscosity of the mixture and the sublayer thickness, and induces drag reduction as observed on prototype (fig. 2). In tunnel spillways, the interactions between the air boundary layer above the flow and the roof affect the air entrainment processes. At the present time, an insufficient number of data is available and additional work is required.

## REFERENCES

- AIVAZYAN, O.M. (1986). "Stabilized Aeration on Chutes." *Gidrotekhnicheskoe Stroitel'stvo*, No. 12, pp. 33-40.
- BOGDEVICH, V.G., EVSEEV, A.R., MLYUGA, A.G., and MIGIRENKO, G.S. (1977). "Gas-Saturation Effect on Near-Wall Turbulence Characteristics." *2nd Intl. Conf. on Drag Reduction*, BHRA Fluid Eng., Cambridge, UK, p. 25.
- CAIN, P. (1978). "Measurements within Self-Aerated Flow on a Large Spillway." Ph.D. Thesis, Uni. of Canterbury, New Zealand.
- CHANSON, H. (1988). "A Study of Air Entrainment and Aeration Devices on a Spillway Model." Research Rep. 88-8, Uni. of Canterbury, New Zealand.
- CHANSON, H. (1992). "Air Entrainment in Chutes and Spillways." Research Report No. CE 133, Dept. of Civil Eng., Univ. of Queensland, Australia.
- CHEPAIKIN, G.A., and DONCHENKO, E.G. (1986). "Certain Effects of Flow Aeration in Spillways." *Gidrotekhnicheskoe Stroitel'stvo*, No. 11, pp. 19-22.
- EHRENBERGER, R. (1926). "Wasserbewegung in steilen Rinnen (Susstennen) mit besonderer Berücksichtigung der Selbstbelüftung." *Zeitschrift des Österreichischer Ingenieur und Architektverein*, No. 15/16 and 17/18.